Peptidylarginine Deiminase Inhibition Prevents Diabetes Development in NOD Mice

Fernanda M.C. Sodré,[1] Samal Bissenova,[1] Ylke Bruggeman,[1] Ronak Tilvawala,[2,3] Dana P. Cook,[1] Claire Berthault,[4] Santanu Mondal,[2] Aïsha Callebaut,[1] Sylvaine You,[4] Raphael Scharfmann,[4] Roberto Mallone,[4,5] Paul R. Thompson,[2] Chantal Mathieu,[1] Mijke Buitinga,[1] and Lut Overbergh[1]

Diabetes 2021;70:516–528 | https://doi.org/10.2337/db20-0421

Protein citrullination plays a role in several autoimmune diseases. Its involvement in murine and human type 1 diabetes has recently been recognized through the discovery of antibodies and T-cell reactivity against citrullinated peptides. In the current study, we demonstrate that systemic inhibition of peptidylarginine deiminases (PADs), the enzymes mediating citrullination, through BB-Cl-amidine treatment, prevents diabetes development in NOD mice. This prevention was associated with reduced levels of citrullination in the pancreas, decreased circulating autoantibody titers against citrullinated glucose-regulated protein 78, and reduced spontaneous neutrophil extracellular trap formation of bone marrow–derived neutrophils. Moreover, BB-Cl-amidine treatment induced a shift from Th1 to Th2 cytokines in the serum and an increase in the frequency of regulatory T cells in the blood and spleen. In the pancreas, BB-Cl-amidine treatment preserved insulin production and was associated with a less destructive immune infiltrate characterized by reduced frequencies of effector memory $CD4^+$ T cells and a modest reduction in the frequency of interferon-γ–producing $CD4^+$ and $CD8^+$ T cells. Our results point to a role of citrullination in the pathogenesis of autoimmune diabetes, with PAD inhibition leading to disease prevention through modulation of immune pathways. These findings provide insight in the potential of PAD inhibition for treating autoimmune diseases like type 1 diabetes.

Emerging evidence demonstrates a role for posttranslational modifications in the pathogenesis of type 1 diabetes (1–10). One of these posttranslational modifications is citrullination, the conversion of arginine into citrulline, mediated by peptidylarginine deiminases (PADs), of which five isozymes have been described (11). The loss of a positively charged arginine in peptides enhances their binding affinity to type 1 diabetes predisposing HLA-DR4 molecules (12,13) and may thereby elicit autoreactive T-cell responses. Indeed, it has been shown that autoreactive $CD4^+$ T cells of patients with type 1 diabetes recognize citrullinated GAD65 (4). Moreover, our group showed that citrullinated glucose-regulated protein 78 (GRP78) is an autoantigen in NOD mice and in human type 1 diabetes (5,6,10). We also provided direct evidence for cytokine-induced citrullination of GRP78 in INS-1E β-cells (5) and human islets (10), indicating that GRP78 can be citrullinated in β-cells in the absence of immune cells. In addition, we showed that inflammatory cytokines induce translocation of GRP78 from the endoplasmic reticulum to the β-cell membrane and its subsequent secretion (5,14), providing the ideal environment to become citrullinated in the extracellular space (15). Although it remains unknown which cells are responsible for protein citrullination in the pancreas, *Padi2* is highly expressed in NOD islets relative to C57BL/6 islets (5,16). Also, increased levels of PAD4 in neutrophils of individuals with type 1 diabetes have been reported (17,18). Interestingly, PAD4 is crucial for the formation of neutrophil extracellular traps (NETs) (19), a process associated with the pathogenesis of type 1 diabetes (20,21). Neutrophils are the first immune cells to infiltrate the islets of NOD mice (20)

[1]Laboratory for Clinical and Experimental Endocrinology, KU Leuven, Leuven, Belgium
[2]Biochemistry and Molecular Pharmacology, University of Massachusetts Medical School, Worcester, MA
[3]Department of Molecular Biosciences, The University of Kansas, Lawrence, KS
[4]Université de Paris, Institut Cochin, CNRS, INSERM, Paris, France
[5]Assistance Publique Hôpitaux de Paris, Hôpitaux Universitaires de Paris Centre-Université de Paris, Cochin Hospital, Service de Diabétologie et Immunologie Clinique, Paris, France

Corresponding author: Lut Overbergh, lutgart.overbergh@kuleuven.be

Received 23 April 2020 and accepted 11 November 2020

This article contains supplementary material online at https://doi.org/10.2337/figshare.13221704.

M.B. and L.O. contributed equally as senior authors.

and have been found in the human pancreas before disease onset (21), with a substantial fraction forming NETs (21). Moreover, various studies targeting neutrophil activity or NETs showed a marked protection against diabetes development in NOD mice (20,22–24).

Citrullination does not occur exclusively in type 1 diabetes. In other autoimmune diseases, citrullinated proteins are present in inflamed target tissues and are associated with the break in immune tolerance (25). In rheumatoid arthritis, for example, citrullinated autoantigens are known to be causative (25). Several studies have reported improved disease outcome without any signs of in vivo toxicity (26–30) using pan-PAD inhibitors, such as Cl-amidine or BB-Cl-amidine, in animal models for rheumatoid arthritis (26,31,32), multiple sclerosis (33), systemic lupus erythematosus (30,34), and ulcerative colitis (27–29). Disease improvement, through direct inhibition of citrullination, was shown to be linked to decreased NET formation (NETosis) (34–37), modulation of dendritic cell function (37), and a shift in Th1/Th2 profiles (31). On the basis of these results, PAD inhibition is gaining interest as a strategy to treat or prevent autoimmune diseases that are associated with abnormal PAD activity.

The mechanism by which BB-Cl-amidine and its mother compound Cl-amidine inactivates PAD has been well described (38). Both compounds irreversibly inactivate PAD enzymes through covalent modification of a conserved cysteine in the active site of the PAD enzymes, thereby having an effect on all PAD enzymes. When PAD enzymes become activated, they undergo a calcium-dependent conformational change that moves a nucleophilic cysteine residue into the active site, and only then, this cysteine is available for the PAD inhibitor (38). Compared with Cl-amidine, BB-Cl-amidine has a longer in vivo half-life (1.75 h vs. ~15 min), a higher cellular potency (half-maximal effective concentration of 8.8 ± 0.6 μmol/L vs. >200 μmol/L for Cl-amidine), and a comparable selectivity for the different PAD enzymes (34). With no reports on the potential efficacy of PAD inhibition in type 1 diabetes models, we here evaluated the effect of BB-Cl-amidine in NOD mice. We observed full protection against diabetes development associated with a decrease in citrullination and in autoantibody titers against citrullinated GRP78. Effects on innate and adaptive immune responses were also observed, with decreased NETosis of bone marrow–derived neutrophils, increased serum Th2 cytokines, and regulatory T cells (T_{reg}) in peripheral tissues and a decrease in effector memory $CD4^+$ T cells (T_{EM}) and interferon-γ (IFN-γ)–producing $CD4^+$ and $CD8^+$ T cells in the pancreas. These findings point to a role for dysregulated PAD activity and citrullination in autoimmune diabetes and provide initial insight into PAD inhibition as a potential therapeutic strategy.

RESEARCH DESIGN AND METHODS

Mice and Treatment Regimen

NOD mice were inbred and housed under semibarrier conditions in our animal facility. Eight-week-old female NOD mice were used. Treatments involved subcutaneous injections with BB-Cl-amidine (1 μg/g body weight) or vehicle (25% DMSO in PBS) six times per week until 25 weeks of age for diabetes incidence or until 13 weeks of age for mechanistic studies (29,31,34,39). Experiments were approved by the institutional animal ethics committee of KU Leuven.

Dispersion of Murine Islets and Sorting

Islets were isolated from 10-week-old NOD mice using collagenase (40). After overnight resting, the islets were dispersed into single-cell suspensions by incubation for 90 s at 37°C in 0.025% trypsin-EDTA (Thermo Fisher Scientific). Cells were surface stained for cell sorting by flow cytometry as previously described (40). A detailed protocol is provided in the Supplementary Material.

RNA Isolation, cDNA Synthesis, and Quantitative PCR

RNA isolation and cDNA generation were performed as previously described (40). SYBR green quantitative PCR was performed on a QuantStudio 3 (Thermo Fisher Scientific) per manufacturer's instructions. Gene expression levels of insulin 1 (*Ins1*), glucagon (*Glc*), *CD45*, *Padi2*, and *Padi4* were normalized to the geometric mean of three housekeeping genes (actin, *RPL27*, and *HPRT*) and analyzed by relative quantification using the $2^{-\Delta Ct}$ method.

Immunohistochemistry

Five-micrometer sections of paraffin-embedded pancreata were collected at 50-μm intervals. Heat-mediated antigen retrieval was performed on deparaffinized sections using citrate buffer (pH 6.1, 20 min; Dako). To detect citrullination, endogenous peroxidase activity was blocked with 0.5% H_2O_2 in methanol for 20 min. Sections were incubated with rabbit anticitrulline (1:50; Abcam) for 1 h and with anti-rabbit horseradish peroxidase (Envision; Dako) for 30 min. Sections were incubated with 3,3′-diaminobenzidine (Dako), counterstained with hematoxylin (2 min), dehydrated, and mounted with DEPEX. For insulin detection, sections were blocked with 10% normal goat serum (Dako) for 20 min and incubated with guinea pig anti-insulin (1:150; Dako) for 1 h and Alexa Fluor 633–conjugated goat anti-guinea pig (1:500; Life Sciences) for 30 min. Sections were counterstained with Hoechst (1:2,000; Thermo Fisher Scientific) and mounted with Mowiol (Polysciences). All incubations were done at room temperature (RT). Imaging was performed using an Olympus BX41 or Zeiss LSM 780 confocal nonlinear optical microscope.

Diabetes Incidence

Mice were tested for clinical signs of diabetes by evaluating glucose levels in the urine with Diastix Reagent Strips (Bayer). As soon as glucosuria was measured, further follow-up was done by measuring blood glucose levels. Mice were considered diabetic when glucosuria was present and blood glucose levels were >200 mg/dL for 2 consecutive days.

Insulitis

At least 25 islets per mouse were scored for lymphocytic infiltration in a blinded manner using hematoxylin-eosin–stained sections.

Insulin Content

Pancreata were homogenized in acidic ethanol (91% ethanol, 9% 1 mol/L H_3PO_4) at 4°C overnight and sonicated. Insulin content was determined in the supernatant by ELISA (Mercodia) and normalized to the weight of the pancreas.

SDS-PAGE and Western Blotting

Protein samples (50 μg) were separated on 4–12% Bis-Tris gels (Invitrogen) and blotted onto polyvinylidene fluoride membranes (Hybond-ECL; GE Healthcare). To detect citrullination, the Anti-Citrulline (Modified) Detection Kit (Millipore) was used. Membranes were incubated with Super-Signal West Femto Maximum Sensitivity Substrate (Thermo Fisher Scientific) and revealed using the ImageQuant LAS 500 system (GE Healthcare). Blots were normalized by reprobing for GAPDH (Thermo Fisher Scientific).

Proteomic Analysis Making Use of Biotin-Phenylglyoxal Labeling

DMSO- ($n = 4$) and BB-Cl-amidine–treated ($n = 4$) mouse pancreata were pooled in buffer (50 mmol/L HEPES, pH 7.6, 0.5% NP40, and 1 mmol/L phenylmethylsulfonyl fluoride) and homogenized using a tissue homogenizer (maximum speed 3 × 20 s at 10-min intervals). The lysed tissue samples were centrifuged (12,000 rpm, 30 min) at 4°C. The supernatants were isolated, and the protein concentration was determined using a detergent compatible assay. Equal protein concentrations from DMSO- and BB-Cl-amidine–treated samples were labeled with biotin-phenylglyoxal (PG) in quadruplicate as previously described (41). A detailed protocol is provided in the Supplementary Material.

Tandem Mass Tag Labeling and Liquid Chromatography Tandem Mass Spectrometry Analysis

A total of eight peptide digests were obtained from quadruplicate biotin-PG labeling of the DMSO- and BB-Cl-amidine–treated samples. The samples were labeled using a tandem mass tag labeling system and prepared for liquid chromatography tandem mass spectrometry (LC-MS/MS) analysis on a nanoACQUITY UPLC (Waters Corporation) coupled to an Orbitrap Fusion Lumos Tribrid (Thermo Fisher Scientific) mass spectrometer. The raw data were processed using Proteome Discoverer version 2.1.1.21 (Thermo Fisher Scientific) and searched against the SwissProt murine (downloaded July 2019) database using Mascot version 2.6.2 (Matrix Science). A detailed protocol is provided in the Supplementary Material.

Autoantibody Assays

Mouse serum autoantibody levels against citrullinated GRP78 were determined by an in-house–developed Meso Scale Discovery (MSD) ELISA. In vitro citrullinated GRP78 was generated as previously described (5). MULTI-ARRAY 96 plates (MSD) were coated (overnight, 4°C) with 5 μg/mL in vitro citrullinated GRP78 in PBS (pH 7) or with 3% skimmed milk in PBS (uncoated control). Blocking was performed with 3% skimmed milk in PBS with 0.5% Tween 20 (2 h at RT). Mouse serum was diluted 1:5 in blocking solution and incubated for 2 h at RT. Wells were incubated for 2 h at RT with SULFO-TAG–labeled goat anti-mouse IgG. Read buffer was added, and detection was done on an MSD reader. To exclude nonspecific signals, each sample had its background signal (serum binding in uncoated well) subtracted from the reading.

NETosis

Bone marrow–derived cells were harvested from the humeri, tibias, and femurs, and neutrophils were isolated using the Neutrophil Isolation Kit (Miltenyi Biotec). Neutrophils were cultured on coverslips precoated with 0.01% Poly L-lysine (Sigma-Aldrich) for 3 h at 37°C in 5% CO_2. Paraformaldehyde-fixed neutrophils were stained with Hoechst (Thermo Fisher Scientific), and NETosis was quantified blindly using a Nikon Eclipse TI microscope. Percentage of NET-releasing cells was calculated by normalizing to the total number of cells. Images were taken on a Zeiss LSM 880 confocal Airyscan microscope.

Cytokine Measurement in Serum

Serum levels of IFN-γ, interleukin (IL)-4, and IL-10 were determined by a single measurement using a V-plex assay from MSD. All concentrations were above the lower limit of detection.

Immune Cell Phenotyping

Blood was incubated three times with NH_4Cl to lyse red blood cells. Single-cell suspensions from spleen were obtained by mechanical disruption, while the pancreas was enzymatically digested for 15 min at 37°C in RPMI medium (72400; Thermo Fisher Scientific) supplemented with 5% bovine serum, 0.05 mmol/L β-mercaptoethanol, 100 units/mL penicillin, 100 units/mL streptomycin, 1 mg/mL collagenase VII, and 0.02 mg/mL DNase I. For phenotypic characterization of T_{reg}, T_{EM}, central memory T-cell (T_{CM}), and naive T-cell (T_{naive}) subsets, cell suspensions were stained using a Zombie Yellow Fixable Viability Kit (BioLegend) and with antibodies against CD4 (BD Biosciences), CD3, CD8, CD44, CD62L, CD25, and Foxp3 (eBioscience). Intracellular staining was performed with Foxp3/Transcription Factor Staining Buffer Set (eBioscience). To evaluate the effect of BB-Cl-amidine treatment on cytokine production, 5×10^5 cells from the spleen and pancreas were stimulated in vitro with 0.025 μg/mL phorbol 12-myristate 13-acetate (PMA) (Sigma-Aldrich) and 0.25 μg/mL ionomycin (Sigma-Aldrich) in the presence of GolgiStop (1:500; BD Biosciences) for 4 h at 37°C in 5% CO_2. Next, cells were incubated with antibodies against CD4 and CD8, treated with Cytofix/Cytoperm (BD Biosciences), and stained with anti-IFN-γ antibody (eBioscience). Samples were acquired on a BD FACS Canto II and analyzed with FlowJo software

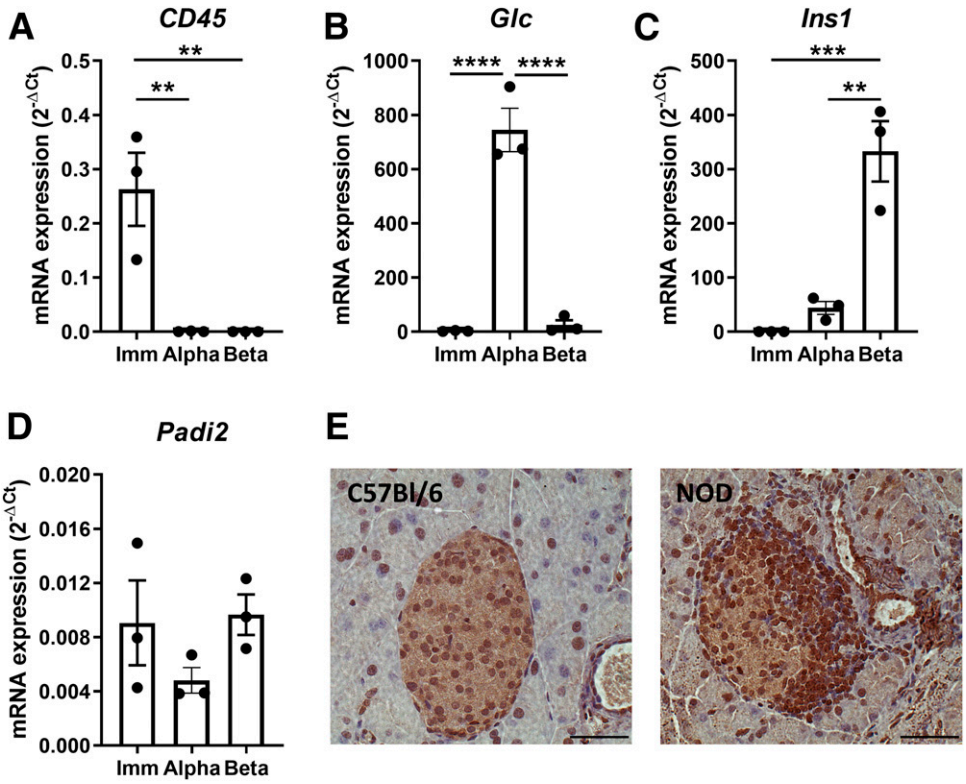

Figure 1—*Padi2* is expressed in immune, α-, and β-cells from NOD islets. *A–D*: mRNA expression level in pancreatic immune cells (Imm), α-cells (Alpha), and β-cells (Beta) for the leukocyte marker *CD45*, α-cell marker glucagon (*Glc*), β-cell marker *Ins1*, and *Padi2* ($n = 3$, three independent experiments were performed with 1 mouse per experiment). *E*: Representative immunohistochemical staining against citrulline in pancreas sections of C57BL/6 and NOD mice (scale bar = 50 μm). All sections where mounted on one slide to enable good comparison. Data in *A–D* are mean ± SEM and were analyzed by one-way ANOVA. $^{**}P < 0.01$, $^{***}P < 0.001$, $^{****}P < 0.0001$.

(TreeStar). The percentage of cytokine-producing cells was determined, and the expression level of the cytokine was assessed using geometric mean fluorescence intensity (MFI). For each experiment, the geometric MFI of each sample was normalized to the average geometric MFI of the DMSO group (MFI fold change).

Statistics

Data were analyzed using GraphPad Prism 8 or Scaffold software. Diabetes incidence was evaluated by Kaplan-Meier survival analysis with Mantel-Cox log-rank test. Data were expressed as mean ± SEM, and after exclusion of outliers, data were analyzed by one-way ANOVA, unpaired *t* test with Welch correction, or Mann-Whitney *U* test, as indicated. $P < 0.05$ was considered statistically significant.

Data and Resource Availability

All data sets generated during the current study are available from the corresponding author upon request.

RESULTS

Pancreatic Islets Express *Padi2* Both in Endocrine and in Infiltrating Immune Cells

Although we have previously shown that islets of 3- and 10-week-old NOD mice have elevated PAD activity levels and enhanced *Padi2* mRNA expression compared with C57BL/6 islets (5), it remains to be elucidated which cell population within the islets is responsible for this high PAD activity. To investigate this, we performed flow cytometry sorting on 10-week-old NOD islet cells, making use of an antibody panel consisting of CD71, CD24, CD49f, and CD45 to enable isolation of highly purified α- and β-cells (40) as well as immune cells. The purity of immune cell fraction was confirmed by marginal expression of *Ins1* and *Glc*. Purity of α- and β-cell fractions was confirmed by complete absence of leukocyte marker *CD45* in both fractions and marginal expression levels of *Glc* (in β-cells) and *Ins1* (in α-cells) (Fig. 1*A–C*). In immune as well as in α- and β-cells, *Padi2* was clearly expressed (Fig. 1*D*), with a trend to higher levels in immune and β-cells compared with α-cells. Of note, *Padi4* mRNA levels were below the detection limit (data not shown). In line with this, immunohistochemical analysis of citrullination in pancreas sections of NOD mice demonstrated intense staining in infiltrated immune cells, while endocrine islet cells stained weakly positive. Parallel staining in age-matched C57BL/6 also showed citrullination in the endocrine islet cells (Fig. 1*E* and Supplementary Fig. 1). These results indicate that citrullination occurs in immune cells infiltrated in the islets and in endocrine α- and β-cells, even in nonpathological conditions.

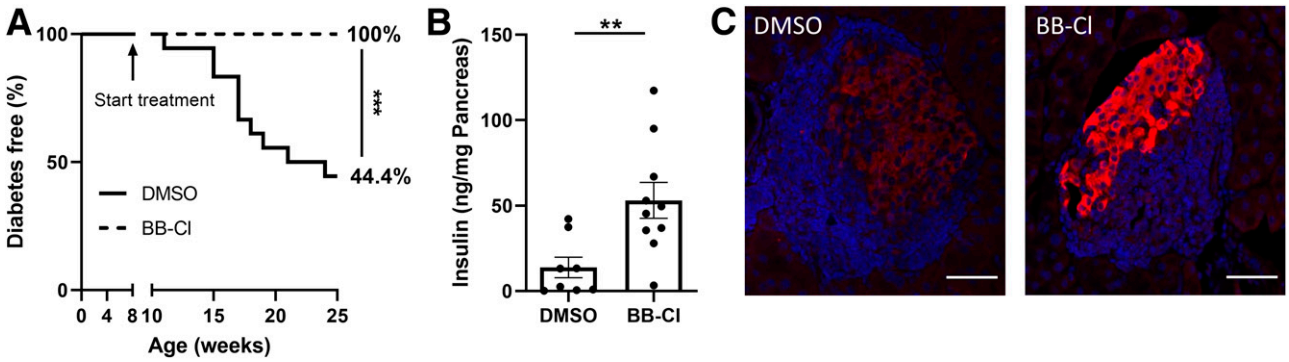

Figure 2—BB-Cl-amidine treatment prevents diabetes development in NOD mice and preserves pancreatic insulin production. *A*: Percentage of diabetes-free NOD mice treated with DMSO or BB-Cl-amidine. Eight-week-old female littermate NOD mice were injected subcutaneously with vehicle (25% DMSO in PBS) or BB-Cl-amidine (1 μg/g body weight) six times per week until 25 weeks of age and followed for diabetes development (n = 17–18 mice per group, two independent cohorts were performed with at least 8 mice per group per experiment). *B*: Pancreatic insulin content of 13-week-old NOD mice treated with DMSO or BB-Cl-amidine from 8 to 13 weeks of age (n = 8–10; two independent experiments were performed with 4–5 mice per group per experiment). *C*: Illustrative images of insulin staining in the pancreata of 13-week-old NOD mice treated from 8 to 13 weeks of age with DMSO or BB-Cl-amidine (scale bar = 50 μm). Data in *A* were evaluated by Kaplan-Meier survival analysis with Mantel-Cox log-rank test. Data in *B* are mean ± SEM and were analyzed by unpaired t test with Welch correction. $^{**}P < 0.01$, $^{***}P < 0.001$.

BB-Cl-Amidine Treatment Prevents Diabetes Development in NOD Mice and Preserves Insulin Production

To examine the role of citrullination on diabetes development, NOD mice were treated with BB-Cl-amidine. Treatment was started at 8 weeks of age, a time point at which insulitis is already ongoing in NOD mice. BB-Cl-amidine treatment fully prevented diabetes development, with all mice free of diabetes until 25 weeks of age, against 44% diabetes free in DMSO-treated mice ($P < 0.001$) (Fig. 2*A*). Therapy was well tolerated as confirmed by normal weight curves (Supplementary Fig. 2). Evaluation of pancreatic insulin content at 13 weeks of age, before the onset of diabetes, showed a fourfold increase of insulin in the pancreata of BB-Cl-amidine–treated mice compared with the control ($P < 0.01$) (Fig. 2*B* and *C*), pointing to preserved insulin production in BB-Cl-amidine–treated mice.

BB-Cl-Amidine Treatment Reduces Citrullination in the Pancreas and Autoantibody Formation Against Citrullinated GRP78

To evaluate the direct effect of BB-Cl-amidine on inhibition of citrullination, we performed immunohistochemical staining of citrullinated protein residues on pancreatic sections, showing a reduced staining intensity in BB-Cl-amidine–treated compared with DMSO-treated mice (Fig. 3*A* and Supplementary Fig. 3). Quantification of the overall level of citrullinated proteins by Western blotting in the pancreata of NOD mice treated with BB-Cl-amidine and vehicle demonstrated that PAD inhibition reduced the total level of protein citrullination by ∼50% ($P < 0.01$) (Fig. 3*B* and *C*). This finding was further confirmed and extended by more quantitative LC-MS/MS analysis. A total of 1,003 citrullinated proteins were identified in pancreata from mice treated with BB-Cl-amidine and vehicle, of which 765 were significantly decreased in abundance by the treatment regimen (Fig. 3*D* and Supplementary Tables 1 and 2). Interestingly, citrullinated GRP78, reported by our group as an autoantigen in murine and human type 1 diabetes (5,10), was the most significantly reduced citrullinated protein, with a decrease of 2.66-fold ($P < 0.0001$). We have previously reported the generation of autoantibodies against citrullinated GRP78 in NOD mice (5). In line with this, we observed here that BB-Cl-amidine treatment decreased autoantibody titers against citrullinated GRP78, both at 13 ($P < 0.05$) (Fig. 3*E*) and at 25 weeks of age ($P < 0.05$) (Fig. 3*F*).

BB-Cl-Amidine Treatment Decreases Spontaneous NETosis in Bone Marrow–Derived Neutrophils

Neutrophils have been suggested to play an important role in the pathogenesis of autoimmune diabetes because they are the first immune cells to infiltrate the islets of NOD mice (20). Also, in patients with type 1 diabetes, neutrophil infiltration is observed in the pancreas, even before disease onset, with some degree of NETosis (21). Since citrullination is a prerequisite for the initiation of NETosis, we questioned here whether BB-Cl-amidine treatment could have an impact on the propensity of neutrophils to form NETs. To this end, spontaneous NETosis was assessed in bone marrow–derived neutrophils isolated from mice treated with BB-Cl-amidine or vehicle. NETosis was significantly reduced in neutrophils from mice treated with BB-Cl-amidine ($P < 0.05$) (Fig. 4). This finding shows that systemic administration of BB-Cl-amidine has an effect on the capacity of neutrophils to form NETs.

BB-Cl-Amidine Alters the Phenotype and Cytokine Production of Immune Infiltrate in the Islets

The finding of preserved insulin production by BB-Cl-amidine led us to investigate the degree and phenotype of immune infiltration. To this end, immunohistochemical

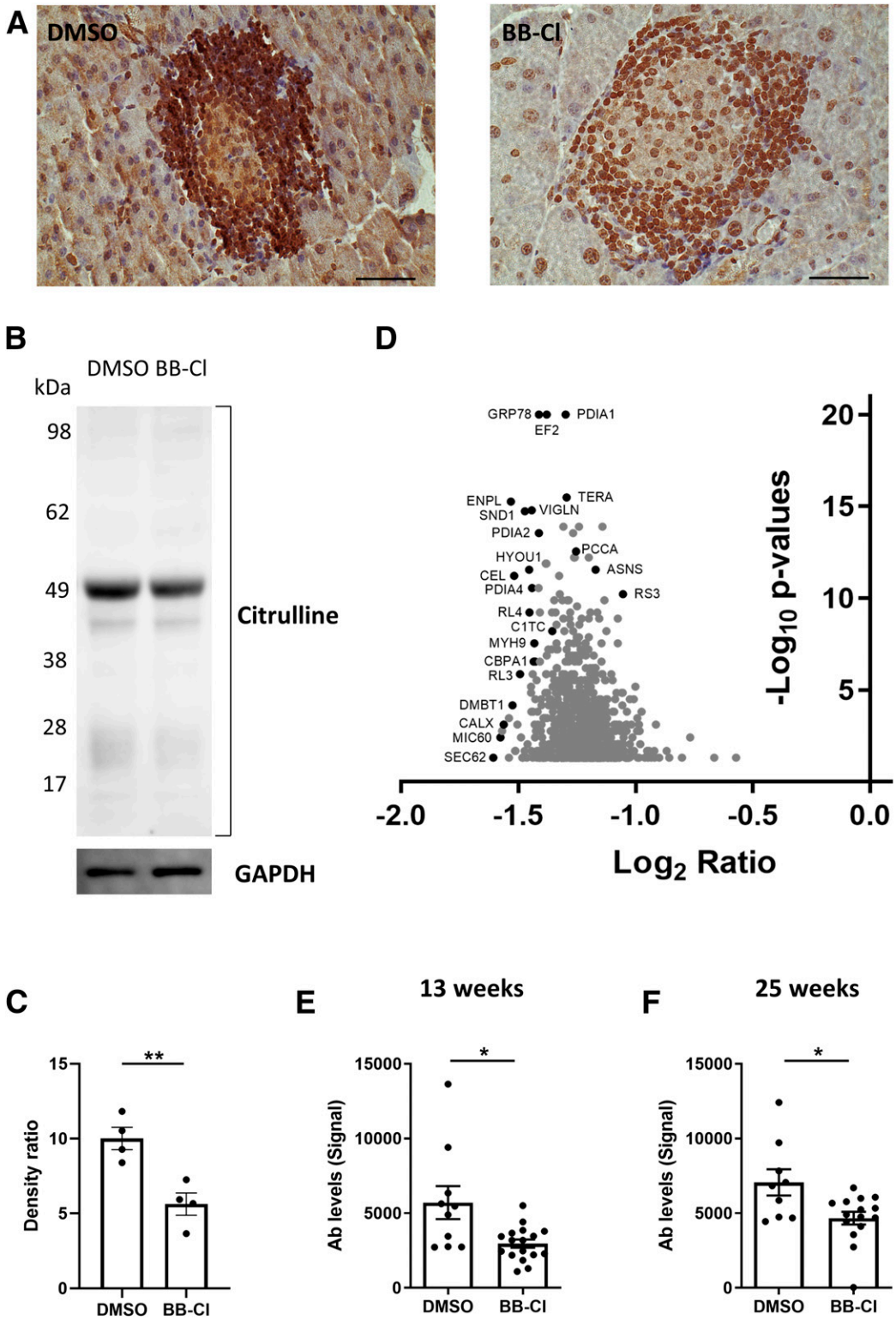

Figure 3—BB-Cl-amidine treatment reduces citrullination in the pancreas and the formation of circulating autoantibodies. *A*: Representative immunohistochemical staining against citrulline in pancreas sections of 13-week-old DMSO- or BB-Cl-amidine–treated NOD mice (scale bar = 50 μm). All sections where mounted on one slide to enable good comparison. *B*: Representative Western blot with anti–modified citrulline antibody in pancreatic lysates of 13-week-old DMSO- or BB-Cl-amidine–treated NOD mice. *C*: Optical density ratio (sum of citrullinated bands/GAPDH band) of pancreas samples from DMSO- or BB-Cl-amidine–treated mice ($n = 4$ mice per group). *D*: Volcano plot showing significant fold changes in citrullinated proteins in pancreata of NOD mice treated with BB-Cl-amidine from 8 until 13 weeks of age compared with DMSO-treated NOD mice. The *x*-axis represents $\log_2$ expression fold changes (BB-Cl-amidine/DMSO), and the *y*-axis represents the adjusted *P* values (as $-\log_{10}$). *E* and *F*: Comparison between the serum levels of anticitrullinated GRP78 antibodies (Ab) in NOD mice treated with DMSO or BB-Cl-amidine at 13 weeks of age and at 25 weeks of age ($n = 9$–17 samples per group; two independent experiments were performed with at least 2 mice per group per experiment). Data in *C*, *E*, and *F* are mean ± SEM and were analyzed by unpaired *t* test with Welch correction. Data in *D* were analyzed by Mann-Whitney *U* test. $^*P < 0.05$, $^{**}P < 0.01$.

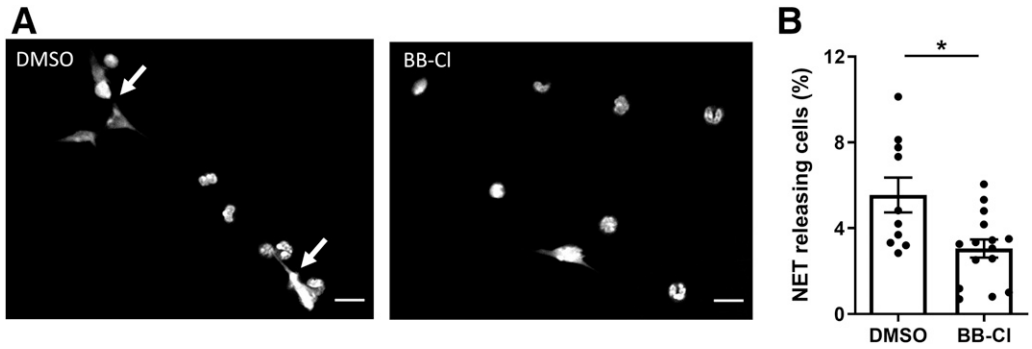

Figure 4— BB-Cl-amidine treatment reduces NET release. *A* and *B*: Bone marrow–derived neutrophils were isolated from 13-week-old NOD mice treated with DMSO or BB-Cl-amidine and cultured for 3 h. Spontaneous NETosis was blindly evaluated by fluorescence microscopy. *A*: Representative images of spontaneous NETosis of bone marrow–derived neutrophils from DMSO- or BB-Cl-amidine–treated mice (scale bar = 10 μm). Arrows point to NET-forming cells. *B*: Percentage of NETosis was quantified blindly by fluorescence microscopy after Hoechst staining (n = 10–15 mice per group; two independent experiments were performed with at least 4 mice per group per experiment). Each dot indicates the value for a single mouse. Data in *B* are mean ± SEM and were analyzed by unpaired t test with Welch correction. *$P < 0.05$.

evaluation of islet immune infiltration at 13 weeks of age showed only a moderate overall decrease of insulitis in the BB-Cl-amidine group (Fig. 5*A*), suggesting a less destructive form of insulitis. To evaluate this further, we measured in vitro cytokine production of the immune cells isolated from the pancreas. Although the overall frequency of IFN-γ–producing T cells was low in both groups, mice treated with BB-Cl-amidine presented a significantly lower percentage of IFN-γ–producing $CD4^+$ and $CD8^+$ T cells ($P < 0.01$ and $P < 0.05$, respectively) (Fig. 5*B* and *C*). Evaluation of the phenotype of immune cells in the pancreas (representative gating strategy in Supplementary Fig. 4*A*) revealed a significant decrease in the percentage of $CD4^+$ T_{EM} cells ($P < 0.05$) (Fig. 5*E*) in BB-Cl-amidine–treated mice, whereas no changes were observed in the frequency of $CD8^+$ T_{EM} and T_{reg} cells (Fig. 5*D*). No differences were observed in $CD4^+$ and $CD8^+$ T_{naive} and T_{CM} subsets (Supplementary Fig. 5). Collectively, these data indicate that although there was only a minor change in the overall level of insulitis, BB-Cl-amidine alters the phenotype of infiltrating immune cells as demonstrated by the decrease in Th1 cytokine production and reduction of T_{EM} locally in the pancreas.

BB-Cl-Amidine Treatment Is Associated With a Th1-to-Th2 Serum Cytokine Shift and With T_{EM} to T_{reg} in the Periphery

Next, we investigated the effect of BB-Cl-amidine treatment on Th1 and Th2 profiles and immune cell phenotypes in the periphery because BB-Cl-amidine has been shown to act through this pathway in other disease models (31). First, we measured serum levels of Th1 and Th2 cytokines in NOD mice treated with BB-Cl-amidine or vehicle. Whereas no significant changes were measured in circulating IFN-γ titers (Fig. 6*A*), IL-4 and IL-10 titers were significantly increased in the BB-Cl-amidine–treated group ($P < 0.01$ for both) (Fig. 6*B* and *C*). This resulted in an overall reduction in the IFN-γ/IL-10 ratio ($P < 0.05$) (42) (Fig. 6*D*). In the spleens of BB-Cl-amidine–treated mice, there was a decrease in IFN-γ production indicated by the reduced frequency of IFN-γ–producing $CD4^+$ T cells ($P < 0.01$) (Fig. 6*E*) as well as the lower expression of IFN-γ in IFN-γ–producing $CD4^+$ and $CD8^+$ T-cell populations ($P < 0.0001$ for both) (Fig. 6*F* and *H*). To specifically investigate the effect on the cellular phenotype of immune cell subsets, we used flow cytometry to study T-cell subsets in the blood and spleen (representative gating strategy in Supplementary Fig. 4*B* and *C*). This revealed that BB-Cl-amidine induced a significant increase in the percentage of T_{reg} in blood ($P < 0.05$) (Fig. 7*A*) and spleen ($P < 0.01$) (Fig. 7*D*). With regard to T_{EM} ($CD4^+$ and $CD8^+$) in the periphery, there was a significant decrease in the percentage of $CD4^+$ T_{EM} cells in the blood and of splenic $CD8^+$ T_{EM} cells ($P < 0.05$ and $P < 0.001$, respectively) (Fig. 7*B* and *F*). No changes were observed in $CD4^+$ and $CD8^+$ T_{CM} populations in the blood and spleen, whereas $CD4^+$ and $CD8^+$ T_{naive} in blood (both $P < 0.05$) (Supplementary Fig. 6*A* and *C*) and $CD8^+$ T_{naive} in spleen ($P < 0.01$) (Supplementary Fig. 6*G*) were increased in BB-Cl-amidine–treated mice. These findings suggest that in the periphery, BB-Cl-amidine induces a shift toward Th2 cytokine production, a decrease in T_{EM}, and an induction of T_{reg}.

DISCUSSION

This study describes the effect of the pan-PAD inhibitor BB-Cl-amidine, showing a complete prevention of diabetes development in NOD mice. This finding highlights the involvement of inflammation-induced citrullination in diabetes development and adds type 1 diabetes to the list of autoimmune diseases in which citrullination participates in disease pathogenesis, a list that includes rheumatoid arthritis (26,31,32), multiple sclerosis (33), lupus (30,34), and ulcerative colitis (27–29). This observation may have significant implications for the development of new

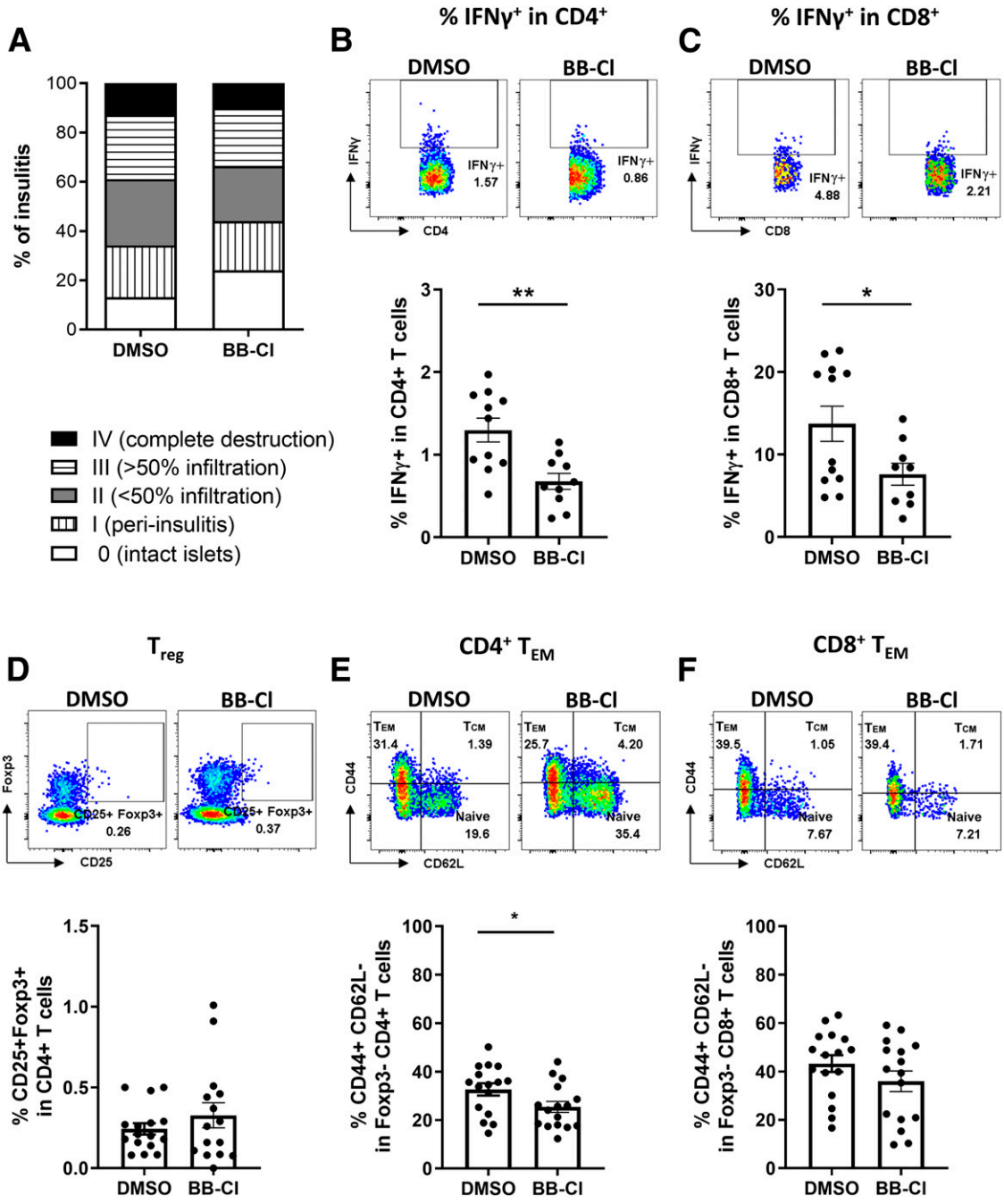

Figure 5—BB-Cl-amidine alters the phenotype of immune infiltrate in the islets. *A*: Insulitis score of 13-week-old NOD mice treated with vehicle (DMSO) or BB-Cl-amidine from 8 to 13 weeks of age ($n = 6$ mice per group; two independent experiments were performed with 3 mice per group per experiment). *B* and *C*: Immune cells isolated from the pancreata of 13-week-old DMSO- or BB-Cl-amidine–treated NOD mice were stimulated in vitro with PMA and ionomycin in the presence of GolgiStop. Representative flow cytometry plots and percentage of IFN-γ–positive cells (%IFNγ$^+$) in CD4$^+$ and CD8$^+$ T cells isolated from pancreas ($n = 9$–12 mice per group; two independent experiments were performed with at least 3 mice per group per experiment). *D–F*: Representative flow cytometry plots and percentage of T_{reg} (CD4$^+$ CD25$^+$ Foxp3$^+$), CD4$^+$ T_{EM} (CD4$^+$ Foxp3$^-$ CD44^{HIGH} CD62L$^-$), and CD8$^+$ T_{EM} (CD8$^+$ Foxp3$^-$ CD44^{HIGH} CD62L$^-$) in pancreata of 13-week-old NOD mice treated with DMSO or BB-Cl-amidine ($n = 15$–16 mice per group; two independent experiments were performed with at least 6 mice per group per experiment). Data in *B–F* are mean ± SEM and were analyzed by unpaired *t* test with Welch correction. *$P < 0.05$, **$P < 0.01$.

therapeutic strategies to mitigate the progression and/or development of type 1 diabetes.

We here provide evidence that the previously reported high expression of *Padi2* in islets of NOD mice (5,16) originates both from the endocrine cells, including α- and β-cells, and from the infiltrating immune cells, thereby conclusively demonstrating that β-cells themselves have the capacity to citrullinate. This finding formed the basis

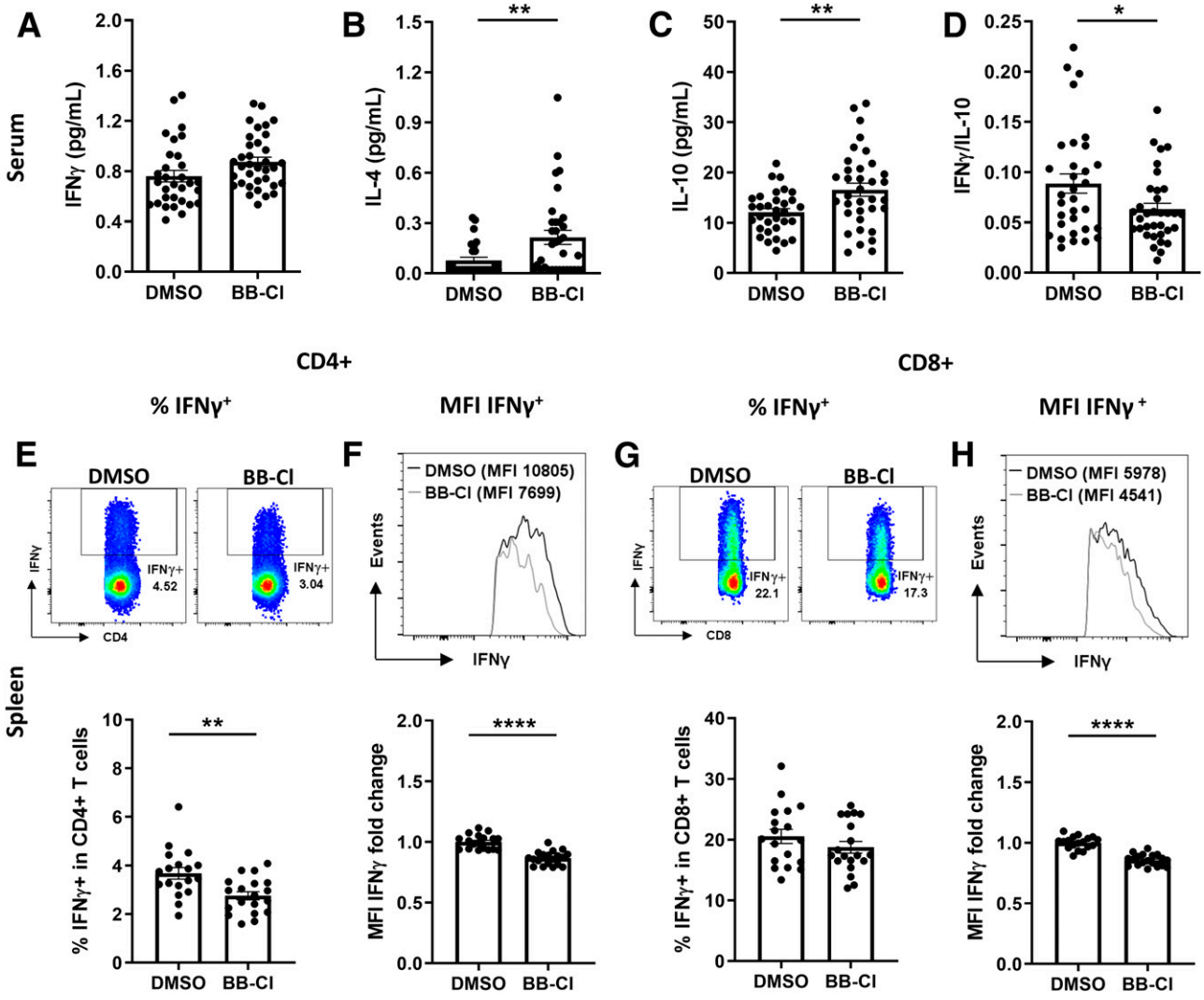

Figure 6—BB-Cl-amidine treatment is associated with a Th1-to-Th2 shift in the periphery. *A–D*: Serum cytokine levels of IFN-γ, IL-4, IL-10, and ratio IFN-γ/IL-10 in 13-week-old NOD mice treated from 8 to 13 weeks with DMSO or BB-Cl-amidine (n = 28–35 mice per group; four independent experiments were performed with at least 7 mice per group per experiment). *E–H*: Splenocytes isolated from the pancreata of 13-week-old DMSO- or BB-Cl-amidine–treated NOD mice were stimulated in vitro with PMA and ionomycin in the presence of GolgiStop (n = 18–19 mice per group; two independent experiments were performed with at least 8 mice per group per experiment). Cytokine production was measured by flow cytometry in $CD4^+$ and $CD8^+$ T-cell populations considering the following two parameters: *1*) percentage of IFN-γ–positive cells (%$IFN\gamma^+$) and *2*) fold change of the MFI of IFN-γ in $IFN\gamma^+$ cells (MFI $IFN\gamma^+$). Per experiment, the geometric MFI of each sample was normalized to the average geometric MFI of the DMSO group. Representative flow cytometry plots and histograms depicting the geometric MFI of IFN-γ between the two groups are shown above the pooled data. *E* and *F*: %$IFN\gamma^+$ and MFI $IFN\gamma^+$ in splenic $CD4^+$ T cells. *G* and *H*: %$IFN\gamma^+$ and MFI $IFN\gamma^+$ in splenic $CD8^+$ T cells. Data are mean ± SEM and were analyzed by unpaired *t* test with Welch correction. $^*P < 0.05$, $^{**}P < 0.01$, $^{****}P < 0.0001$.

for evaluating the effect of PAD inhibition in NOD mice. In the current treatment regimen, we started treatment at 8 weeks of age, a time point at which insulitis is already ongoing. The observation that inhibition of PAD activity, and thus citrullination, protected NOD mice against diabetes development suggests that citrullination may play a role in the amplification of the disease rather than being an initial trigger in breaking of immune tolerance. This strengthens our earlier findings of minor autoreactivity against citrullinated GRP78 in prediabetic NOD mice (5) and the increased occurrence of autoantibodies and autoreactive T-cell responses in patients with long-standing type 1 diabetes versus those with new-onset diabetes (10). This view also fits well with the knowledge that citrullination is mostly associated with inflammation, thereby playing a role in several autoimmune diseases where citrullination takes place in the inflamed target tissues (26–34). The low levels of citrullination in islets of C57BL/6 mice further demonstrate that citrullination is present already under physiological conditions; however, the degree of citrullination is markedly increased in NOD islets associated with immune infiltration.

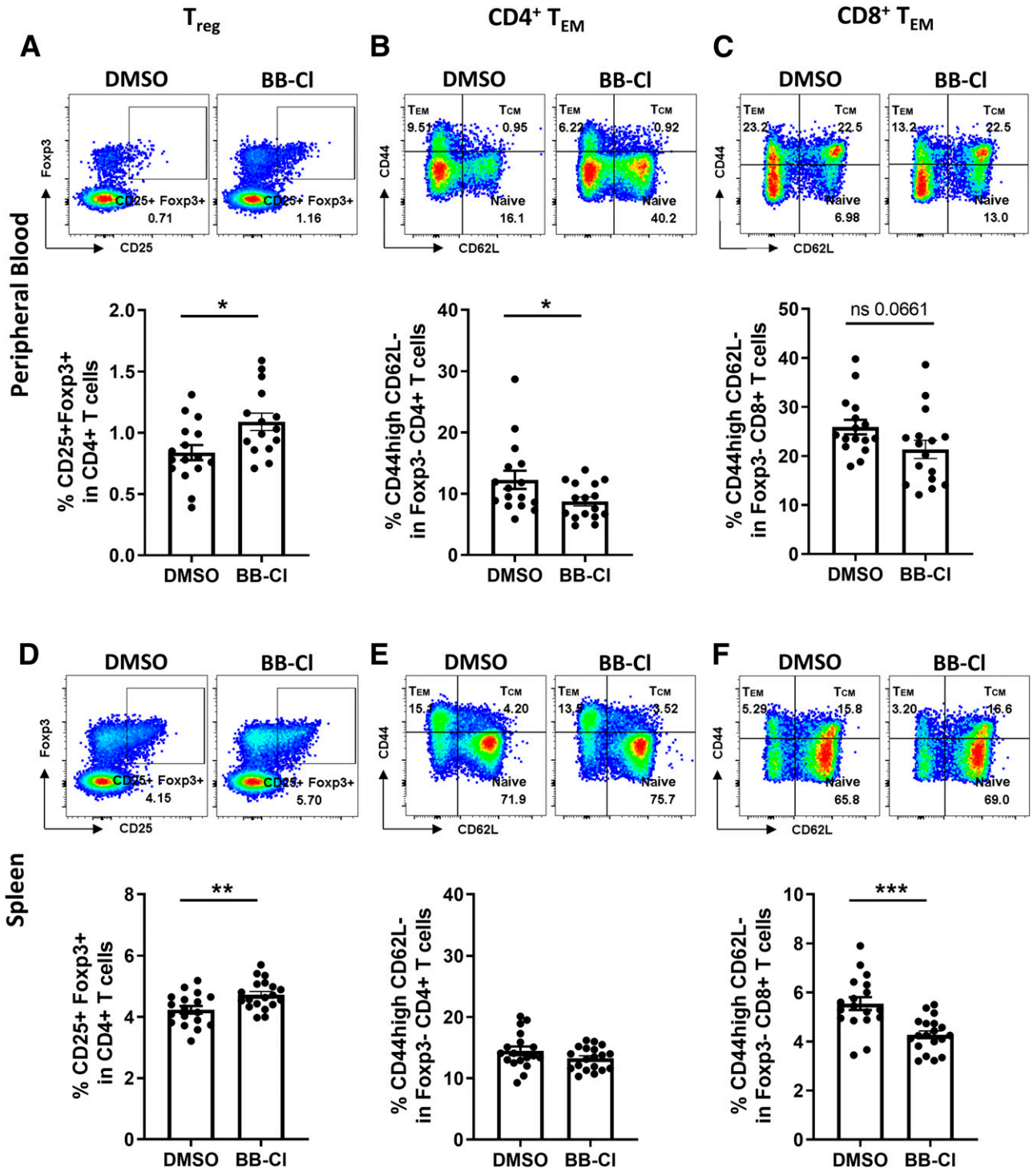

Figure 7—BB-Cl-amidine increases the frequency of T_{reg} in the periphery. Representative flow cytometry plots and percentage of T_{reg} ($CD4^+$ $CD25^+$ $Foxp3^+$), $CD4^+$ T_{EM} ($CD4^+$ $Foxp3^-$ $CD44^{HIGH}$ $CD62L^-$), and $CD8^+$ T_{EM} ($CD8^+$ $Foxp3^-$ $CD44^{HIGH}$ $CD62L^-$) in peripheral blood (*A–C*) and spleen (*D–F*) from 13-week-old NOD mice treated with DMSO or BB-Cl-amidine (n = 15–19 mice per group; two independent experiments were performed with at least 6 mice per group per experiment). Data are mean ± SEM and were analyzed by unpaired t test with Welch correction. *$P < 0.05$, **$P < 0.01$, ***$P < 0.001$. ns, not significant.

BB-Cl-amidine treatment is effective in decreasing overall levels of citrullination in the pancreas, as shown by Western blotting and quantitative LC-MS/MS. Of interest, the most significant reduction was measured for citrullinated GRP78. In line with this, the level of autoantibodies against citrullinated GRP78 is decreased in the circulation of BB-Cl-amidine–treated NOD mice. Although autoantibodies are not believed to be pathogenic in type

1 diabetes, this finding underlines the important effect of BB-Cl-amidine on reducing the antigenicity of β-cell proteins in the inflamed islet environment.

Pan-PAD inhibitors are known to alter NET release (34–37). Neutrophils and NETosis are believed to play an important role in the initiation and perpetuation of type 1 diabetes (20,21,43). Here, we show that BB-Cl-amidine reduces spontaneous NET release ex vivo from bone marrow–derived neutrophils of NOD mice, a finding that may be linked to a decrease in citrullinated histone H3 levels. Indeed, citrullination of histone H3, mediated by activation of PADs in neutrophils, is an initiating factor for the formation of NETs (44) and has been shown to be reduced by PAD inhibition (36). Our results are in line with studies in lupus (30,34) and collagen-induced arthritis (37), demonstrating that reduced NETosis in response to PAD inhibition is associated with disease amelioration.

Looking at the islet level, BB-Cl-amidine treatment resulted in only a marginal reduction of insulitis, whereas pancreatic insulin levels were preserved. However, we did observe a significant reduction in the percentage of $CD4^+$ T_{EM} and in the frequency of IFN-γ–producing $CD4^+$ and $CD8^+$ T cells in the pancreata of BB-Cl-amidine–treated mice. The observed reduction in IFN-γ production may reflect an impaired effector function of the infiltrating immune cells (45). These results suggest that the immune cell infiltrate in BB-Cl-amidine–treated mice is less aggressive (46).

Our results on increased frequency of T_{reg} in the blood and spleen demonstrate a peripheral effect of BB-Cl-amidine. Additionally, splenic IFN-γ production of BB-Cl-amidine–treated mice was significantly reduced. These results suggest a more regulatory environment that favors immune tolerance and prevents intensification of the immune assault. Also, with Th1/Th2 polarization believed to play a role in type 1 diabetes pathogenesis, the significant increase in IL-4 and decrease in the IFN-γ/IL-10 ratio in the circulation of BB-Cl-amidine–treated mice supports this hypothesis. Of note, whether Th1/Th2 polarization is a cause rather than a consequence of disease development is not fully established. In line with these findings, an induction of Th2 cells by BB-Cl-amidine has been shown in a mouse model of rheumatoid arthritis (31), and a direct effect of PAD inhibition on enhancing the differentiation of Th2 subsets through inhibition of GATA3 citrullination was demonstrated mechanistically by Sun et al. (47).

For the first time, a pan-PAD inhibitor was used in a very long treatment regimen (17 weeks), with no detrimental side effects observed. This, together with reported disease amelioration with the use of PAD inhibitors in other autoimmune models, opens the road to potential clinical therapeutic applications. However, since PADs also participate in physiological processes (11), such as gene regulation and nerve myelination, such therapeutic treatment regimens will need careful consideration. The recent development of specific PAD2 (48) and PAD4 (49) inhibitors, as well as reversible PAD inhibitors (50), may be a solution, but their efficacy to treat autoimmune diseases remains to be confirmed. Results from ongoing studies may further invite to consider PAD inhibition as a therapeutic strategy not only for type 1 diabetes but also for other autoimmune diseases.

In conclusion, treatment of NOD mice with BB-Cl-amidine resulted in complete diabetes prevention associated with decreased protein citrullination, anticitrulline autoantibody formation, NETosis, and in situ IFN-γ responses. We postulate that these effects, combined with the direct effect of PAD inhibition on T cells, might lead to a less aggressive inflammatory environment in the islets and in the periphery. Our findings align with previous reports that citrullination plays a pathogenic role in type 1 diabetes and demonstrate that PAD inhibition is an attractive target for clinical therapeutic applications in autoimmunity.

Acknowledgments. The technical assistance of Eline Desager, Jos Laureys, Marijke Viaene, and Martine Gilis (Laboratory of Clinical and Experimental Endocrinology, KU Leuven) is greatly appreciated. The authors thank the KU Leuven Flow Cytometry Core Facility for assistance with flow cytometry. Fluorescent images were recorded on a Zeiss LSM 780–SP Mai Tai HP DeepSee (Cell and Tissue Imaging Cluster supported by Hercules AKUL/11/37 and FWO G.0929.15 to Pieter Vanden Berghe, University of Leuven) or on a Zeiss LSM 880–Airyscan (Cell and Tissue Imaging Cluster supported by Hercules AKUL/15/37_GOH1816N and FWO G.0929.15 to Pieter Vanden Berghe, University of Leuven). The authors thank the University of Massachusetts Medical School proteomics core facility director Dr. Scott Shaffer for helping with proteomics analysis and Dr. Roshanak Aslebagh for running proteomics samples.

Funding. This work was supported by IMI2-JU under grant agreements 115797 (INNODIA) and 945268 (INNODIA HARVEST). This joint undertaking receives support from the European Union's Horizon 2020 research and innovation program and European Federation of Pharmaceutical Industries and Associations, JDRF, and The Leona M. and Harry B. Helmsley Charitable Trust. Further support came from the KU Leuven (C16/18/006), Fonds voor Wetenschappelijk Onderzoek Vlaanderen (a predoctoral fellowship for S.B. [11A0220N], D.P.C. [11Y6716N], and A.C. [1189518N] and a postdoctoral fellowship for M.B. [12R0719N]), and the National Institutes of Health (R35-GM-118112 to P.R.T.).

Duality of Interest. No potential conflicts of interest relevant to this article were reported.

Author Contributions. F.M.C.S. contributed to the study design and conduct and analysis and interpretation of the data and wrote and edited the manuscript. S.B. helped with the design, conduct, and analysis of the NETosis data. Y.B. contributed by injecting mice and performing experiments. R.T. and P.R.T. conducted and analyzed the proteomic analysis of the biotin-PG–labeled samples and the LC-MS/MS. D.P.C. helped with mice treatment and contributed to the design and analysis of the FACS data. C.B. and R.S. performed and analyzed the islet isolation, sorting, and quantitative PCR. S.M. and P.R.T. provided the BB-Cl-amidine. A.C. helped with conducting experiments. S.Y. and R.M. contributed to the design and interpretation of islet experiments. C.M., M.B., and L.O. designed the research, interpreted data, and wrote and edited the manuscript. M.B. also conducted and analyzed experiments. All authors edited the manuscript and gave their final approval of the version to be published. C.M. and L.O. are the guarantors of this work and, as such, had full access to all the data in the study and take responsibility for the integrity of the data and the accuracy of the data analysis.

References

1. Mannering SI, Harrison LC, Williamson NA, et al. The insulin A-chain epitope recognized by human T cells is posttranslationally modified. J Exp Med 2005;202:1191–1197

2. Delong T, Baker RL, He J, Barbour G, Bradley B, Haskins K. Diabetogenic T-cell clones recognize an altered peptide of chromogranin A. Diabetes 2012;61: 3239–3246
3. van Lummel M, Duinkerken G, van Veelen PA, et al. Posttranslational modification of HLA-DQ binding islet autoantigens in type 1 diabetes. Diabetes 2014;63:237–247
4. McGinty JW, Chow IT, Greenbaum C, Odegard J, Kwok WW, James EA. Recognition of posttranslationally modified GAD65 epitopes in subjects with type 1 diabetes. Diabetes 2014;63:3033–3040
5. Rondas D, Crèvecoeur I, D'Hertog W, et al. Citrullinated glucose-regulated protein 78 is an autoantigen in type 1 diabetes. Diabetes 2015;64:573–586
6. Babon JAB, DeNicola ME, Blodgett DM, et al. Analysis of self-antigen specificity of islet-infiltrating T cells from human donors with type 1 diabetes. Nat Med 2016;22:1482–1487
7. Strollo R, Vinci C, Napoli N, Pozzilli P, Ludvigsson J, Nissim A. Antibodies to post-translationally modified insulin as a novel biomarker for prediction of type 1 diabetes in children. Diabetologia 2017;60:1467–1474
8. Marre ML, McGinty JW, Chow IT, et al. Modifying enzymes are elicited by ER stress, generating epitopes that are selectively recognized by $CD4^+$ T cells in patients with type 1 diabetes. Diabetes 2018;67:1356–1368
9. Gonzalez-Duque S, Azoury ME, Colli ML, et al. Conventional and neoantigenic peptides presented by β cells are targeted by circulating naïve CD8+ T cells in type 1 diabetic and healthy donors. Cell Metab 2018;28:946–960.e6
10. Buitinga M, Callebaut A, Marques Câmara Sodré F, et al. Inflammation-induced citrullinated glucose-regulated protein 78 elicits immune responses in human type 1 diabetes. Diabetes 2018;67:2337–2348
11. Witalison EE, Thompson PR, Hofseth LJ. Protein arginine deiminases and associated citrullination: physiological functions and diseases associated with dysregulation. Curr Drug Targets 2015;16:700–710
12. Nguyen H, James EA. Immune recognition of citrullinated epitopes. Immunology 2016;149:131–138
13. McGinty JW, Marré ML, Bajzik V, Piganelli JD, James EA. T cell epitopes and post-translationally modified epitopes in type 1 diabetes. Curr Diab Rep 2015;15: 90
14. Vig S, Buitinga M, Rondas D, et al. Cytokine-induced translocation of GRP78 to the plasma membrane triggers a pro-apoptotic feedback loop in pancreatic beta cells. Cell Death Dis 2019;10:309
15. Zhou Y, Chen B, Mittereder N, et al. Spontaneous secretion of the citrullination enzyme PAD2 and cell surface exposure of PAD4 by neutrophils. Front Immunol 2017;8:1200
16. Crèvecoeur I, Gudmundsdottir V, Vig S, et al. Early differences in islets from prediabetic NOD mice: combined microarray and proteomic analysis. Diabetologia 2017;60:475–489
17. Wong SL, Demers M, Martinod K, et al. Diabetes primes neutrophils to undergo NETosis, which impairs wound healing. Nat Med 2015;21:815–819
18. You Q, He DM, Shu GF, et al. Increased formation of neutrophil extracellular traps is associated with gut leakage in patients with type 1 but not type 2 diabetes. J Diabetes 2019;11:665–673
19. Wang Y, Li M, Stadler S, et al. Histone hypercitrullination mediates chromatin decondensation and neutrophil extracellular trap formation. J Cell Biol 2009;184: 205–213
20. Diana J, Simoni Y, Furio L, et al. Crosstalk between neutrophils, B-1a cells and plasmacytoid dendritic cells initiates autoimmune diabetes. Nat Med 2013;19: 65–73
21. Vecchio F, Lo Buono N, Stabilini A, et al.; DRI_Biorepository Group; Type 1 Diabetes TrialNet Study Group. Abnormal neutrophil signature in the blood and pancreas of presymptomatic and symptomatic type 1 diabetes. JCI Insight 2018;3: e122146
22. Citro A, Valle A, Cantarelli E, et al. CXCR1/2 inhibition blocks and reverses type 1 diabetes in mice. Diabetes 2015;64:1329–1340
23. Liang Y, Wang X, He D, et al. Ameliorating gut microenvironment through staphylococcal nuclease-mediated intestinal NETs degradation for prevention of type 1 diabetes in NOD mice. Life Sci 2019;221:301–310
24. Shu L, Zhong L, Xiao Y, et al. Neutrophil elastase triggers the development of autoimmune diabetes by exacerbating innate immune responses in pancreatic islets of non-obese diabetic mice. Clin Sci (Lond) 2020;134: 1679–1696
25. Alghamdi M, Alasmari D, Assiri A, et al. An overview of the intrinsic role of citrullination in autoimmune disorders. J Immunol Res 2019;2019:7592851
26. Kawaguchi H, Matsumoto I, Osada A, et al. Peptidyl arginine deiminase inhibition suppresses arthritis via decreased protein citrullination in joints and serum with the downregulation of interleukin-6. Mod Rheumatol 2019;29:964–969
27. Chumanevich AA, Causey CP, Knuckley BA, et al. Suppression of colitis in mice by Cl-amidine: a novel peptidylarginine deiminase inhibitor. Am J Physiol Gastrointest Liver Physiol 2011;300:G929–G938
28. Witalison EE, Cui X, Causey CP, Thompson PR, Hofseth LJ. Molecular targeting of protein arginine deiminases to suppress colitis and prevent colon cancer. Oncotarget 2015;6:36053–36062
29. Chumanevich AA, Chaparala A, Witalison EE, et al. Looking for the best anticolitis medicine: a comparative analysis of current and prospective compounds. Oncotarget 2017;8:228–237
30. Knight JS, Zhao W, Luo W, et al. Peptidylarginine deiminase inhibition is immunomodulatory and vasculoprotective in murine lupus. J Clin Invest 2013;123: 2981–2993
31. Kawalkowska J, Quirke AM, Ghari F, et al. Abrogation of collagen-induced arthritis by a peptidyl arginine deiminase inhibitor is associated with modulation of T cell-mediated immune responses. Sci Rep 2016;6:26430
32. Willis VC, Gizinski AM, Banda NK, et al. N-α-benzoyl-N5-(2-chloro-1-iminoethyl)-L-ornithine amide, a protein arginine deiminase inhibitor, reduces the severity of murine collagen-induced arthritis. J Immunol 2011;186:4396–4404
33. Moscarello MA, Lei H, Mastronardi FG, et al. Inhibition of peptidyl-arginine deiminases reverses protein-hypercitrullination and disease in mouse models of multiple sclerosis. Dis Model Mech 2013;6:467–478
34. Knight JS, Subramanian V, O'Dell AA, et al. Peptidylarginine deiminase inhibition disrupts NET formation and protects against kidney, skin and vascular disease in lupus-prone MRL/lpr mice. Ann Rheum Dis 2015;74:2199–2206
35. Madhi R, Rahman M, Taha D, Mörgelin M, Thorlacius H. Targeting peptidylarginine deiminase reduces neutrophil extracellular trap formation and tissue injury in severe acute pancreatitis. J Cell Physiol 2019;234:11850–11860
36. Biron BM, Chung C, Brien XMO, Chen Y, Reichner J, Ayala A. Cl-amidine prevents histone 3 citrullination and neutrophil extracellular trap formation, and improves survival in a murine sepsis model. J Innate Immun 2018;9:22–32
37. Papadaki G, Kambas K, Choulaki C, et al. Neutrophil extracellular traps exacerbate Th1-mediated autoimmune responses in rheumatoid arthritis by promoting DC maturation. Eur J Immunol 2016;46:2542–2554
38. Luo Y, Arita K, Bhatia M, et al. Inhibitors and inactivators of protein arginine deiminase 4: functional and structural characterization. Biochemistry 2006;45: 11727–11736
39. Ghari F, Quirke AM, Munro S, et al. Citrullination-acetylation interplay guides E2F-1 activity during the inflammatory response. Sci Adv 2016;2:e1501257
40. Berthault C, Staels W, Scharfmann R. Purification of pancreatic endocrine subsets reveals increased iron metabolism in beta cells. Mol Metab 2020;42: 101060
41. Tilvawala R, Nguyen SH, Maurais AJ, et al. The rheumatoid arthritis-associated citrullinome. Cell Chem Biol 2018;25:691–704.e6
42. Schloot NC, Hanifi-Moghaddam P, Goebel C, et al. Serum IFN-γ and IL-10 levels are associated with disease progression in non-obese diabetic mice. Diabetes Metab Res Rev 2002;18:64–70

43. Valle A, Giamporcaro GM, Scavini M, et al. Reduction of circulating neutrophils precedes and accompanies type 1 diabetes. Diabetes 2013;62:2072–2077
44. Jorch SK, Kubes P. An emerging role for neutrophil extracellular traps in noninfectious disease. Nat Med 2017;23:279–287
45. Bhat P, Leggatt G, Waterhouse N, Frazer IH. Interferon-γ derived from cytotoxic lymphocytes directly enhances their motility and cytotoxicity. Cell Death Dis 2017;8:e2836
46. Mallone R, van Endert P. T cells in the pathogenesis of type 1 diabetes. Curr Diab Rep 2008;8:101–106
47. Sun B, Chang HH, Salinger A, et al. Reciprocal regulation of Th2 and Th17 cells by PAD2-mediated citrullination. JCI Insight 2019;4:e129687
48. Muth A, Subramanian V, Beaumont E, et al. Development of a selective inhibitor of protein arginine deiminase 2. J Med Chem 2017;60:3198–3211
49. Lewis HD, Liddle J, Coote JE, et al. Inhibition of PAD4 activity is sufficient to disrupt mouse and human NET formation. Nat Chem Biol 2015;11:189–191
50. Aliko A, Kamińska M, Falkowski K, et al. Discovery of novel potential reversible peptidyl arginine deiminase inhibitor. Int J Mol Sci 2019;20:2174